J. Embryol. exp. Morph. 97, 125–139 (1986)
Printed in Great Britain © *The Company of Biologists Limited 1986*

Electrical properties of the otic vesicle epithelium in the chick embryo

J. J. REPRESA, E. BARBOSA AND F. GIRALDEZ

Depto. Anatomía and Depto. Fisiología y Bioquímica, Facultad de Medicina, Universidad de Valladolid, 47005 Valladolid, Spain

SUMMARY

The electrophysiological properties of the epithelium of the otic vesicle were studied in the chick embryo using conventional microelectrode techniques. A preparation is described that allows continuous recording of transmural potential and resistance during changes in the composition of the bathing fluid. Vesicles in stages 18 to 22 showed a spontaneous transmural potential (E_T) that ranged from 2 to 6 mV, inner positive. This electrical potential difference was abolished after 2 h incubation in K^+-free strophantidin (10^{-4} M) and it increased by about twofold immediately after addition of the cation ionophore Amphotericin B (250 μM) to the bath. The specific resistance of the wall (R_T) was about 80 Ωcm^2 between stages 18 and 22 indicating a low-resistance, noncellular, permeation pathway for current flow. The short-circuit current, calculated from E_T and R_T was about 50×10^{-6} A cm^{-2} throughout this period. This corresponds to a net flux of 187×10^{-8} mol $cm^{-2} h^{-1}$ of a single cation pumped towards the vesicular cavity. Diffusion potentials (salt gradients and single-ion substitutions) showed a selectivity ratio $P_K : P_{Na} : P_{Cl} = 1 : 0{\cdot}9 : 0{\cdot}7$, which is that of a weakly charged aqueous pathway. Measurements of vesicular volume and surface area showed an increase by a factor of ten in the size of the vesicle with maximal rates of change in volume of 5 $\mu l\, cm^{-2} h^{-1}$. The electrical properties reported here for the epithelium of the otic vesicle resemble very much those of 'leaky' epithelia which are known to transport ions and water at a very high rate.

INTRODUCTION

The early development of the inner ear in the vertebrates involves the thickening and invagination of the ectodermal layer and the formation of the otic vesicle (see Romanoff, 1960). The wall of the vesicle consists of a pseudostratified epithelium with some structural features of transporting epithelia (Valdecasas *et al.* 1977), but whose functional properties have not been studied. Ionic gradients and fluxes are known to be of importance in development (see Warner, 1983) and transepithelial transport appears to play specific roles during early ontogenesis. For instance, there is evidence suggesting that isotonic transport of ions and water is responsible for the generation of blastocoele fluid in the mammalian and amphibian embryo (Smith, 1970; Cross, 1973; Slack & Warner, 1973, 1975). Active sodium transport and fluid secretion have been recently demonstrated in the epiblast of chick embryos by Stern & MacKenzie (1983) and Stern, Manning & Gillespie (1985). These authors suggest a role for transepithelial ion transport in the regulation of cell polarity and in the formation of the third embryonic layer.

Key words: otic vesicle, ion transport, epithelial transport, chick embryo.

Transepithelial transport could be therefore involved in cavity formation and may represent a general mechanism regulating volume, pressure and, or, composition of closed extracellular spaces. With this in mind we have investigated here the basic electrical properties of the epithelium of the otic vesicle. This was done by using microelectrodes and conventional techniques for potential recording and current injection on a semi-isolated vesicle preparation. The results show that the otic vesicle is a low-potential, low-resistance epithelium with a dominant paracellular ion-permeation pathway. These properties resemble very much those of 'leaky' epithelia which are known to perform isotonic fluid transport. A preliminary account of this work has been previously published (Barbosa, Giraldez & Represa, 1985).

MATERIALS AND METHODS

General

Experiments were done on chick embryos (Strain-Cross) obtained from fertilized eggs that were incubated at 38·5°C. Embryos were explanted into a Petri dish containing standard physiological saline (see below) and fixed with entomological pins to the floor of the dish which had been filled with carbon paraffin. The amnion was opened with fine scissors under the microscope and the embryo staged according to Hamburger & Hamilton (1951). Embryos in developmental stages 16 to 24 were used for this work. At this time, the otic vesicle appears as a bilateral spheroidal structure, located dorsally at the level of the branchial arches. It is surrounded by mesenchyme and covered superficially by the ectoderm. In order to expose the otic vesicle it was necessary to remove this layer carefully. Using fine tungsten needles, two parallel incisions were made in the ectoderm, prolonging dorsally the direction of the first and second branchial clefts. They were joined by a third incision at the base of the second arch that produced an ectodermal flap which could be reflected to give direct access to the vesicle. The procedure left a semi-isolated otic vesicle held in position by the surrounding mesenchyme. Embryos were usually bisected through the sagittal plane to improve visualization during the experiment. The surgical procedure was done at room temperature and with frequent renewal of the bathing solution. The specimen was then transferred to the experimental chamber which is schematically represented in Fig. 1A. This consisted of a ring (8 mm height, 15 mm diameter) cut from a plastic 10 ml syringe and glued to a microscope slide. The floor was covered with Sylgard to allow fixation with small pins. The preparation could then be visualized under a binocular microscope. Fig. 1B shows a typical preparation. The solution that bathed the vesicle could be continuously renewed by superfusing the preparation with fresh solution flowing under gravity. A three-way valve allowed alteration of the incoming solution. The volume of the chamber was about 0·7 ml and the solution could be completely exchanged in less than 15 s as judged from measurements done with ion-selective microelectrodes after a tenfold change in concentration.

Solutions

The standard bathing solution contained (mM): Na^+, 120; K^+, 2; Ca^{2+}, 1; Mg^{2+}, 1; Cl^-, 126. In some experiments the ionic composition of the solution was modified by isotonic replacements. In low-NaCl solution (12 mM-NaCl) NaCl was diluted to one-tenth by substitution with sucrose. Na^+ was isotonically replaced by K^+ in high-K^+ solution (120 mM-KCl). In some experiments the following additions were made to the standard solution: ouabain (10^{-3} M), strophantidin (10^{-5} M), Amphotericin B (25×10^{-7} M), dinitrophenol (6×10^{-4} M) and sodium cyanide (10^{-3} M). All solutions were buffered with Tris 5 mM titrated to a pH of 7·4.

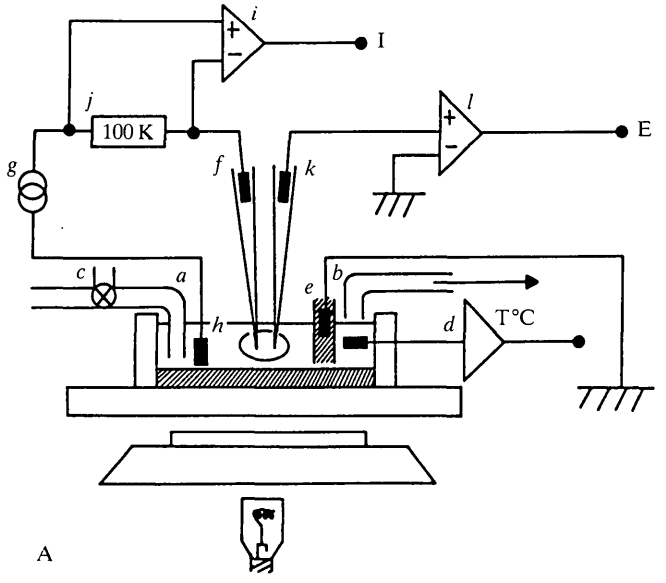

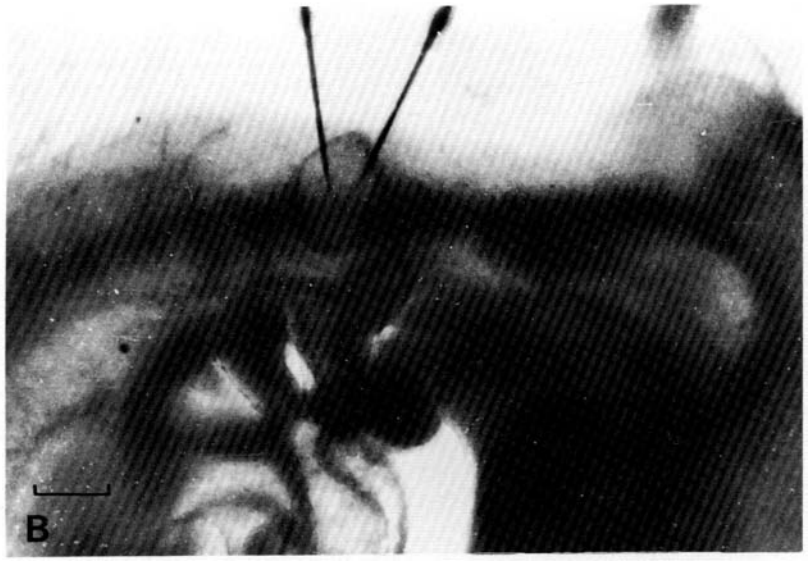

Fig. 1. (A) Experimental chamber and electrical arrangements. The otic vesicle was perfused with fluid coming from *a*, running under gravity, and the fluid was collected by suction at *b*. The bathing solution could be changed by the operation of the valve *c*. Temperature was controlled electronically at *d*. The bath electrode *e* was a 3 M-KCl agar bridge connected through an Ag^+:AgCl halfcell to ground and placed downstream, close to the outlet. The current-injecting microelectrode is represented by *f*. A floating current source *g* was used to inject current into the vesicle. The current sink was an Ag^+:AgCl pellet (*h*) and the current was measured with a differential amplifier *i* from the voltage drop across the resistor *j*. The voltage-measuring microelectrode *k* was connected to an electrometer *l*. (B) Photograph of the semi-isolated preparation as it is seen during experiments with microelectrodes. In the centre, between the dorsum and the branchial arches, the otic vesicle can be distinctly seen. The ectoderm covering the vesicle has been dissected to give ready access to the otocyst. Two microelectrodes are seen after impalement. They were dipped in ink to better visualize the tips. The preparation was lightly stained with neutral red to improve the image. The photograph was taken at ×20. Bar, 100 μm.

Microelectrodes

Transmural potential and resistance was measured using glass microelectrodes. Pipettes were pulled from borosilicate glass tubing, 1·5 mm o.d. and 0·9 mm i.d., in a two-stage horizontal puller. Tip resistances were initially about 30 MΩ when filled with 3 M-KCl or 4 M-potassium acetate and measured in the standard physiological saline. Electrodes were always bevelled after pulling, so to reduce their resistances to 5–10 MΩ, by means of a thick-slurry beveller based on the design of Lederer, Spindler & Eisner (1979). This improved the performance of microelectrodes for current injection and also reduced tip potentials to less than 0·5 mV which was critical here, given the small potentials to be measured.

Electrical arrangements

The basic electrical circuit is depicted schematically in Fig. 1A. Electrode *k* was connected to an electrometer (input impedance, 10^{11} ohms) and was used to measure potentials. Electrode *f* was used to inject current. Square-wave current pulses (500 ms, up to 10^{-6} A) were passed through the microelectrode from a stimulus isolation unit which was driven by a stimulator. The current source was virtually ground-free and a large load resistance (10^8 ohms), served to convert the pulses into approximately constant current pulses. The actual current flowing through the circuit and being injected to the vesicle could be measured as the voltage drop across a 10^5 ohm resistor with a differential electrometer. Potentials and currents were displayed on an oscilloscope and continuously recorded on a two-channel pen recorder. In some cases, signals were also stored on a four-channel FM-magnetic tape.

The second electrode was used in a few instances to inject dyes into the vesicles. This was done by connecting the microelectrode, filled with a solution containing the dye, to a syringe through a polyethylene tube filled with mineral oil. Fast green (FCF) and alcian blue were used in these experiments at a final concentration of 2 %.

Measurement of vesicular surface area and volume

Embryos used for morphometric studies were fixed in Carnoy or Bouin solutions and embedded in paraffin. The blocks were cut serially at 8 μm, stained in haematoxylin–eosin and mounted with Caedax. The external contour of the vesicle in each section was drawn with a camera lucida at ×40. The length of the perimeter was then measured and stored in a computer that could be programmed to calculate the volume and surface area of the reconstructed vesicle. In order to estimate the degree of distortion introduced by the fixation and embedding procedures on the measurements of vesicular volume, the shrinkage factor (SF) was calculated following the technique described by Zilles (1978). The fresh otocyst was drawn with the camera lucida. The specimen was then processed and the vesicle drawn again under the same magnification. Volumes were calculated and SF, i.e. the volume of the processed vesicle as a fraction of the fresh one, was obtained. The figures for stages 18 and 21 (at the steepest portion of the growth curve, see Fig. 5) were 0·82 and 0·84 respectively indicating that the measurements on processed material might underestimate the values by a small fraction (15–20 %). This fraction is constant throughout the period studied in this paper therefore retraction does not distort the growth curve of vesicular volume. The effect of shrinkage was therefore ignored in this work.

Diffusion potentials

Dilution potentials (salt gradients) and bi-ionic potentials (single ionic substitutions) were generated by the appropriate ionic substitutions and analysed according to the Plank–Henderson formalism (see Crone, 1984). For the case of two different solutions of the same salt (NaCl), the electrical potential difference is given by:

$$E^D = -\frac{RT}{F}\frac{1-\gamma}{1+\gamma}\ln\frac{c_{in}}{c_{out}} \quad (1)$$

where γ is the ratio P_{Cl^-}/P_{Na^+}, c_{in} and c_{out} the concentrations inside and outside the vesicle and

R, T and F have their usual meaning. The equation for two solutions of two different salts with a common anion (KCl: NaCl) is:

$$E^B = -\frac{RT}{F} \ln \frac{1+\beta}{\alpha+\beta} \tag{2}$$

where β is the ratio P_{Cl^-}/P_{K^+} and α the ratio P_{Na^+}/P_{K^+}. Absolute permeability coefficients were then calculated from:

$$P_i = -\frac{RT}{(zF)^2} \cdot \frac{g_i}{c_i} \tag{3}$$

where P_i is the individual ionic permeability coefficient, and g_i the partial ionic conductance. As discussed by Crone (1984) the calculated junction potentials between electrodes filled with concentrated KCl solutions and 150 mM solutions of KCl or NaCl are very small. Actual changes in potential at the reference (bath) electrode were measured in the experimental chamber under conditions similar to the experiment but connecting the input of the electrometer to the bath through a 3 M-KCl agar-bridge or a broken-tip microelectrode. The change in potential upon flowing low-NaCl or high-K^+ solutions was, in such conditions, less than 0·3 and 0·1 mV respectively. These changes are small compared to those measured across the vesicular wall and were disregarded in the calculations of ionic permeabilities.

RESULTS

Measurement of transepithelial potential and resistance

In the following experiments the electrical potential and resistance across the wall of the otic vesicle was measured with two microelectrodes. The technique is illustrated in Fig. 2 where a successful impalement of a vesicle is shown. At the arrow labelled *a* the voltage-recording electrode (upper trace) was moved forward and by inspection it was seen to penetrate the vesicular wall. At the same time the positive-going deflection in the voltage trace in the record was observed. It then levelled at about 4 mV and remained constant throughout the period of observation. Sometimes, especially with fine electrodes ($R > 10\,M\Omega$), a fast negative-going transient was recorded before the trace stabilized at a positive potential. We attributed this first transient to the incomplete penetration of cells in the wall. At arrow *b*, a current-injecting electrode penetrated the wall producing transient changes in the voltage recording that were synchronous with the current pulses (lower trace), indicating that a resistance was now interposed between the tip of the microelectrode and ground. At *c* the second electrode was withdrawn and at *d* the same was done with the voltage-recording electrode. It can be seen that the voltage trace returned to the original baseline without any appreciable drift. Conventional impalement criteria used in microelectrode work (Giraldez, 1984) are seen to be fulfilled here: (1) sharp deflexion on entry, (2) stability and (3) return to the original baseline upon withdrawal, without appreciable drift. The additional requirement of no change in the electrode tip resistance during and after the impalement was also regularly used. The rationale behind this is that, given the low impedance of the vesicular wall as compared to that of the microelectrode (50 kΩ *versus* 10 MΩ), the latter should not change upon penetration of the vesicle unless obstructed.

Further assessment of the intravesicular location of the microelectrode was made in some cases by pressure injection of dyes, fast-green FCF and alcian blue, through the microelectrode. These were seen to diffuse within the vesicular cavity in a few seconds. The diffusional barrier for each dye, however, seemed to be located at a different place. Fast green was seen to diffuse rapidly across the epithelial wall to appear at the outer limit of the vesicle, at the level of the location of the basal membrane. Alcian blue, on the other hand, remained within the vesicular cavity, without appreciable leak across the wall. This suggests that transepithelial permeation is not completely free but limited by the junctional complexes between cells (see below).

All vesicles that were successfully impaled according to the criteria described above, produced spontaneous transmural potential differences (E_T) that ranged from 2 to 6 mV (inner positive). On average, E_T was $3{\cdot}7 \pm 0{\cdot}3$ mV in 27 vesicles between stages 18 to 22. Vesicles corresponding to embryos in stage 16–17 showed lower potentials ($2{\cdot}5 \pm 0{\cdot}6$ mV) and no electrical potential difference could be recorded from vesicles in stage 15.

In order to get an indication of the origin of the recorded transmural potential, we studied the effects of some drugs which are known to affect transport in

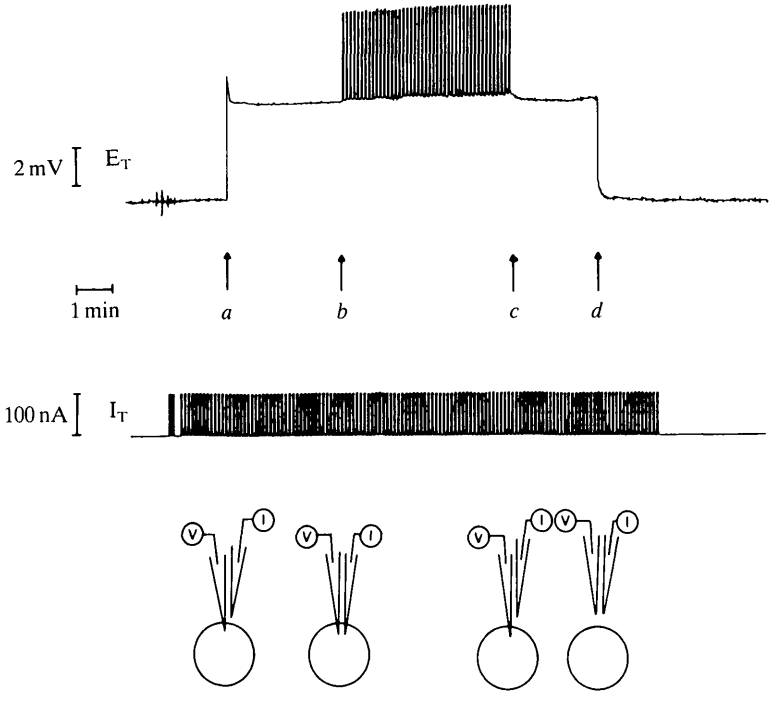

Fig. 2. Transmural potential and resistance in the otic vesicle. The upper trace shows the electrical potential (E_T) and the lower trace the current injected through a second microelectrode (I_T). The letters correspond to the four situations djagrammatically shown in the bottom of the figure. Calibrations are shown at the left. The time scale is common for both recordings. The experiment was done on a semi-isolated vesicle (experiment no. 2284.3) at stage 20.

epithelia. Metabolic inhibitors, dinitrophenol and cyanide, and Na^+-pump inhibitors, strophantidin and ouabain, did not have any immediate effect on transepithelial potential. No attempt was made to inject these substances into the vesicle. However, long incubations under conditions in which the sodium pump is inhibited, for instance 2 h in Ringer containing zero K^+ plus 10^{-4} M-strophantidin, abolished the transepithelial potential difference. Cardiac glycosides are known to permeate very slowly across intercellular junctions. This observation therefore, along with the sign of the transepithelial potential (inner positive) would be consistent with a model in which internally located Na^+,K^+-pumps were generating the electrical difference. With this view in mind, the nonselective cation ionophore, Amphotericin B was then used to stimulate the Na^+-pump by loading the cells with Na^+ (see Cremaschi, Henin, Meyer & Bacciola (1977) and Reuss (1978)). The effect of this drug was to increase E_T as illustrated by the experiment in Fig. 3 in which Amphotericin B (final concentration = 250 μM) was added to the bath whilst transmural potential was recorded. E_T can be seen to increase very rapidly, becoming more positive by about twofold, and then to decay during the remaining 10–15 min. The indication is then that E_T can be augmented by stimulation of Na^+ transport through the Na^+-pump.

Transepithelial resistance

The electrical resistance of the vesicular wall gives an idea of the restrictions imposed to the exchange with the external medium. The input resistance of the vesicles (R_i, Ω) was measured from the voltage drop for constant current pulses, as shown before in Fig. 2. Fig. 4A shows the average values of the input resistance throughout development. This increased from zero to about 50 kΩ between stages 16 and 18 and then fell to 10 kΩ by stages 23–24. The current–voltage relation was approximately linear for moderate voltage displacements (±20 mV) as illustrated by the experiment in Fig. 4B. This shows the instantaneous current–voltage relationship obtained from a vesicle in stage 19. The slope of the line gives a

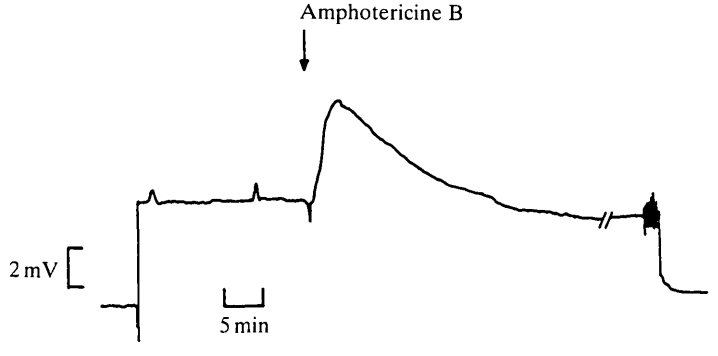

Fig. 3. Effects of Amphotericin B on transepithelial potential. The recording shows the impalement of an otic vesicle with a microelectrode and the continuous recording of E_T. The arrow indicates the application of Amphotericin B (250 μM). Calibrations are shown at the left. Experiment no. 19685; stage 19.

measure of the resistance of the dominant pathway. Further displacements of potential about E_T (± 20 mV) were not produced because, owing to the low resistance of the vesicles, these would have required delivery of too large currents through the microelectrode.

In order to calculate the specific resistance of the epithelium (R_T, Ωcm^2), the surface area of the vesicles was measured at each developmental stage using standard morphometric techniques, as described in the Materials and Methods section. The results are shown in Fig. 5A,B. It can be noted that there is a rapid and pronounced increase in the vesicular volume and surface area taking place between stages 19 and 22. The slope of the volume curve is a measure of the rate of change in vesicular volume, being maximal during stages 20–21 and about $2 \times 10^{-6} cm^3 h^{-1}$.

Assuming a uniform current density, the specific resistance of the wall was calculated as $R_T = R_i \cdot S$ (Ωcm^2); the values are shown in Fig. 6. R_T is seen to rise between stages 16 and 18 to level at about 80 Ωcm^2 from then onwards. The equivalent short-circuit current, calculated at each stage from the values of E_T and R_T is shown in the inset of Fig. 6. It was, on average, about 50×10^{-6} A cm^{-2}

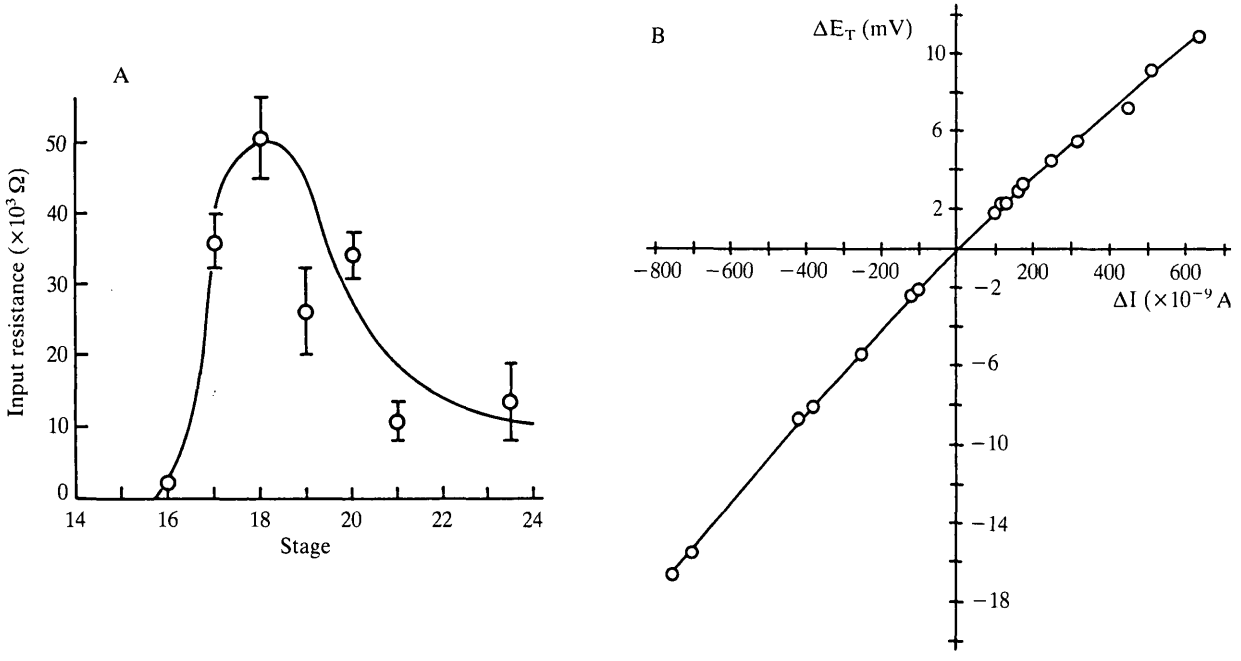

Fig. 4. Input resistance of the otic vesicle. (A) Vesicular input resistance as a function of development. Input resistance, measured from the voltage drop for constant current pulses from experiments as in Fig. 2, is plotted against the developmental stage. Points are means of three to eight experiments and the bars represent the standard error. (B) Current–voltage relation in the otic vesicle. The change in transmural potential (ordinates) is plotted against the injected current. Current was injected as current pulses of different sign and amplitude (500 ms duration, 0·2 Hz). The line was drawn by eye. The slope ($\Delta V/\Delta F$) represents the input resistance, R_i (Ω). Experiment no. 17584, stage 19.

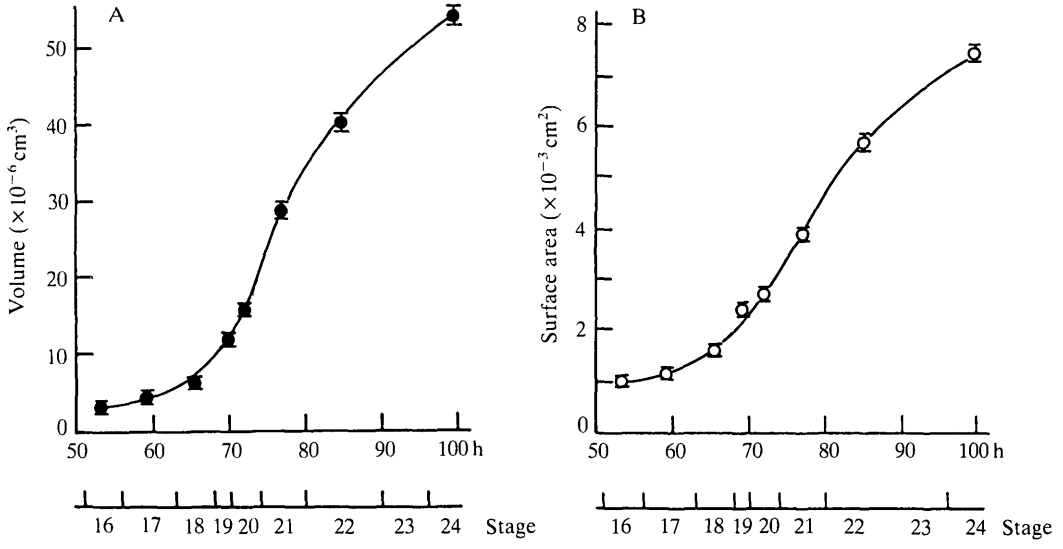

Fig. 5. Vesicular volume and surface area throughout development. Vesicular volume (A) and the vesicular surface area (B) were measured from serial reconstructions of vesicles as described in Materials and Methods. Points represent means of four measurements and the bars indicate S.E. The lines were drawn by eye.

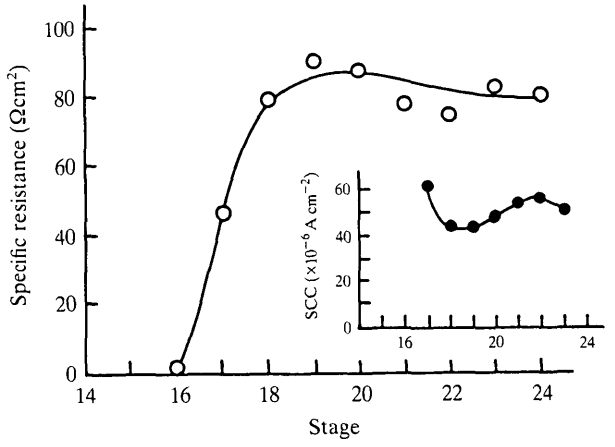

Fig. 6. Specific resistance and short-circuit current as a function of development. The specific resistance, calculated from the input resistance and the vesicular surface, is plotted against the corresponding developmental stage. The inset shows the values of the short-circuit current (I_{SC}) calculated from E_T/R_T for each stage.

throughout the period between stages 18 and 22. Under the assumption of symmetry in the solutions, this represents a net inward current in the absence of electrochemical potential gradient, corresponding to a net flux of 187×10^{-8} mol $cm^{-2}\,h^{-1}$ of a single cation pumped towards the vesicular cavity.

Diffusion potentials

The results described above point to a dominant paracellular pathway for current flow in the vesicular epithelium. It seemed therefore of interest to

characterize the ionic selectivity of this pathway by measuring potentials and resistances after altering the ionic composition of the bathing fluid. Examples of bi-ionic and dilution potentials generated across the vesicular wall are shown in Fig. 7. The replacement of Na^+ by K^+ (120 mM-KCl) produced a small, positive-going change in transepithelial potential with a small decrease in the total resistance (Fig. 7A), indicating a similar conductance for these two cations. The reduction of NaCl to 12 mM by isotonic substitution with sucrose (Fig. 7B) led to a change in E_T of 5 to 8 mV, becoming interior-negative with respect to the bath. A simultaneous increase in transmural resistance to about twice its initial value is observed, suggesting that both Na^+ and Cl^- permeate across the epithelium and that Na^+ diffuses faster than Cl^-. Results of several experiments are summarized in Table 1. The Plank–Henderson equation for diffusion potentials can be used to calculate the permeability coefficients of the paracellular pathway. Using equations *1* and *2* (Materials and Methods) and the values of Table 1, the selectivity pattern is $P_K:P_{Na}:P_{Cl} = 1:0{\cdot}9:0{\cdot}7$ and the corresponding transference numbers in the standard solution are 0·01, 0·56 and 0·43. The absolute ionic permeabilities, calculated from these values and equation (3) of the Materials and Methods section, are ($\times 10^{-6}$ cm s^{-1}): $P_K = 1{\cdot}6$, $P_{Na} = 1{\cdot}4$ and $P_{Cl} = 1{\cdot}1$. This pattern indicates the existence of a poorly selective, weakly charged permeation pathway presumably associated with the intercellular junctions.

DISCUSSION

The present experiments were aimed at establishing the basic electrical properties of the wall of the otic vesicle. A method was developed to measure transmural potential and resistance from semi-isolated vesicles under continuous perfusion with solutions of different composition. The results show that: (1) otic vesicles produce spontaneous transmural potentials of about 4 mV (inner positive), (2) this potential can be altered by drugs acting on the Na^+,K^+-pump, (3) transmural resistances of about 80 Ωcm^2 and equivalent short-circuit currents of 50 A cm^{-2} can be measured after the closure of the vesicle and its isolation from the ectoderm (stage 18) and (4) the selectivity pattern of the epithelial wall is that of a large, weakly charged aqueous channel. We now briefly consider the significance and possible limitations of these findings.

Conventional criteria for the acceptance of impalements with microelectrodes were used here. The small magnitude of the transmural potential generated by the otic vesicle, a feature in common with all fluid transporting epithelia, forced us to be especially cautious. For instance, microelectrodes were always bevelled before use in order to reduce their tip resistance and, even more important, to minimize their tip potential. Given the low transepithelial resistance of the otocyst, it is very likely that, in the steady state, the ionic composition of the vesicular fluid is similar to that of the external bath. With such low tip potentials and similar ionic compositions it seems very improbable that the recorded potentials were caused by changes in the liquid-junction potential at the tip of the microelectrode. The

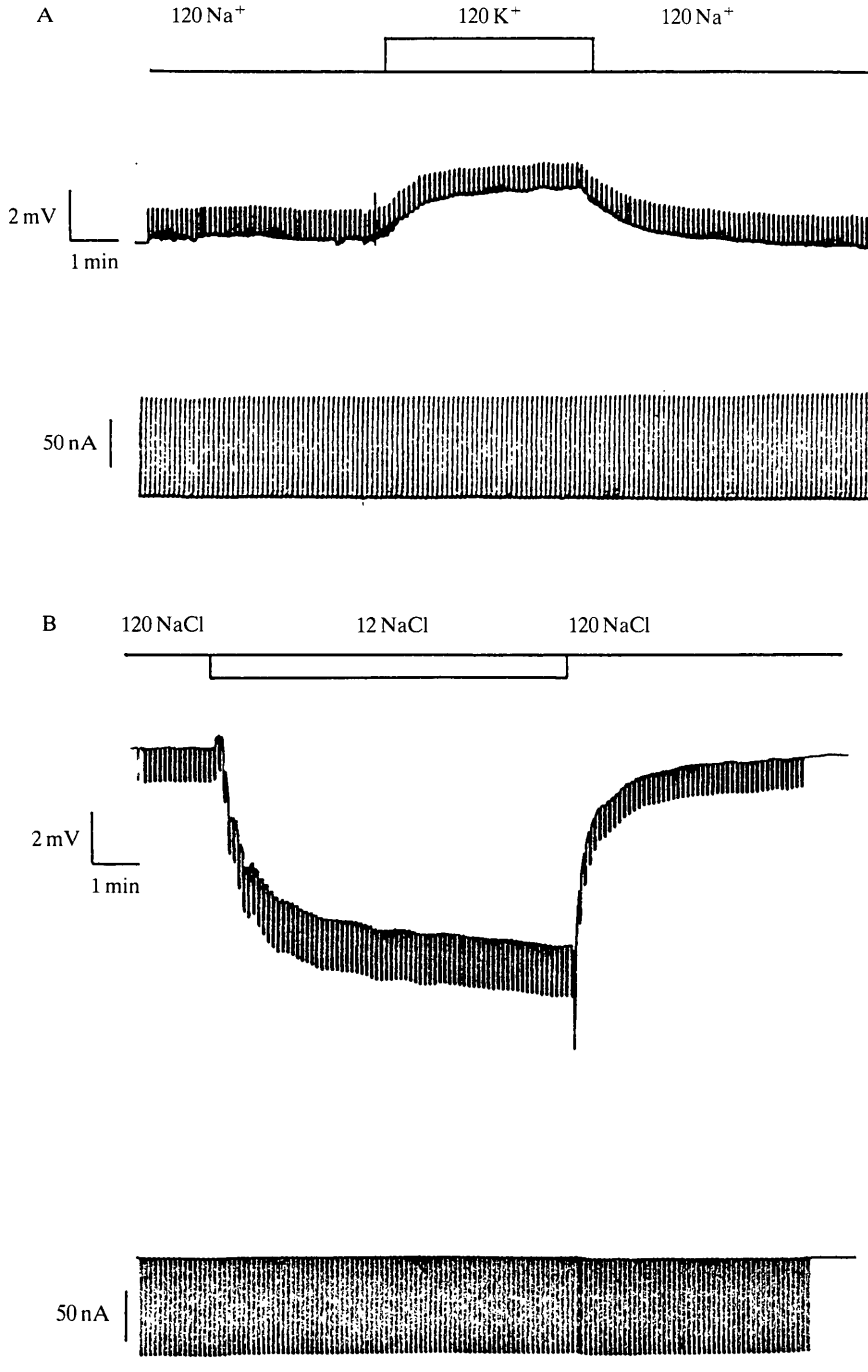

Fig. 7. Diffusion potentials across the otic vesicle. (A) Effects of high-K^+ solutions on E_T and R_T. The record starts with two microelectrodes inside the vesicle to measure E_T (upper trace) and I_T (lower trace). Note that the size of the deflexions in E_T are proportional to the transmural resistance. During the period indicated by the upper bar the standard Ringer (120 Na^+, 2 K^+ (mM)) was substituted by high-K^+ solution (120 K^+ + 2 Na^+ (mM)). Experiment no. 8584.1, stage 20. (B) Effects of low-NaCl solutions on E_T and R_T. Recording of E_T and I_T as in A. The upper bar indicates the period in which NaCl was diluted to 1:10 by partial (equimolar) replacement by sucrose. Experiment no. 8584.2, stage 20+.

Table 1. *Transepithelial diffusion potentials in the otic vesicle*

	Control		Experimental			
	E_T (mV)	R_T (Ωcm^2)	E_T (mV)	R_T (Ωcm^2)	ΔE_T (mV)	ΔR_T (Ωcm^2)
High-K^+	4·1 ± 0·7	57 ± 8	5·8 ± 0·8	47 ± 7	1·8 ± 0·4	−10 ± 7
Low-Na^+	4·0 ± 0·4	59 ± 9	−1·9 ± 0·7	125 ± 27	−5·9 ± 0·5	66 ± 18

Data obtained in experiments like shown in Fig. 7 from vesicles in stages 18–20. Numbers are mean ± standard error of six experiments. High-K^+ solution = 120 KCl + 2 NaCl (mM) and low-Na^+ solution = 12 NaCl (mM) plus sucrose to isotonicity. $E_T = E_{T(experimental)} - E_{T(control)}$.

intravesicular location of the microelectrode tip was assessed by (1) visual inspection, seeing how the microelectrode penetrated the wall, (2) the appearance of a voltage drop upon inserting a second, current-injecting, microelectrode and (3) the injection of dyes through a second microelectrode. Taken together, these observations indicate that there is a spontaneous electrical potential difference across the vesicular wall. The time-dependent appearance of the transepithelial resistance in parallel with the development of E_T also supports this view.

These basic electrical properties of the vesicular epithelium, a low-potential low-resistance epithelium, resemble very much those of a category of epithelia referred to as 'leaky' epithelia, which are known to transport ions and water at a very high rate (Fromter & Diamond, 1970). An interesting possibility is, therefore, that the vesicular potential is a transport potential originated by the activity of the cells. This would be supported by the inhibitory effect of K^+-free strophantidin solutions and the stimulatory effect of the cation ionophore Amphotericin B. Although the results are consistent with a two-membrane model with internally located Na^+ pumps, this view requires more direct experimental evidence. The effect of drugs on transepithelial potentials have always to be assessed with care because, as shown by Lew, Ferreira & Moura (1979), the origin of the transepithelial potential is a complex function of diffusional fluxes across each one of the cell membranes in series, electrogenic pump-mediated fluxes and junctional ionic fluxes in parallel. The effect of a given inhibitor might be difficult to see if, as it is most likely, the contribution of the Na^+-pump to the transmural potential is low and the time for the dissipation of the ionic gradients is long. The lack of effect of metabolic inhibitors seen here as well as that reported by others in the amphibian blastocoel (Slack & Warner, 1973) could have this origin. Similarly, in *Necturus* gall bladder, a typical 'leaky' epithelium, the transepithelial potential remains almost unchanged after 1 h incubation in a medium containing ouabain (1 mM) (Reuss, Bello-Reuss & Grady, 1979; Giraldez, 1984).

The low transmural resistance measured in the otic vesicle indicates that transepithelial current flow is dominated by a 'shunt', paracellular, pathway (see Fromter & Diamond, 1970). The results from ion-substitution experiments show that individual ionic permeabilities for the major monovalent ions (Na^+, K^+ and

Cl^-) are large and also that the selectivity of the filter is rather poor. The mobility pattern clearly deviates from the sequence in free solution, anions being relatively excluded, suggesting the presence of weak, negatively charged sites. These are properties of the paracellular pathway described in typical 'leaky' epithelia such as intestine (Frizzell & Schultz, 1972), proximal tubule (Boulpaep, 1971; Frömter, Muller & Wick, 1971) and gall bladder (Frömter, 1972; Frizzell, Dugas & Schultz, 1975). Most probably, these are properties dependent on the organization of the 'tight' junctions for it is unlikely that intercellular spaces could impose any restriction to ion movements (Frömter, 1972).

The suggestion of a fluid transport function for the vesicular epithelium is of interest and it would imply a role for transepithelial ion transport in this structure. It is important, therefore, to establish the relation between ion transport and vesicular growth (volume) throughout development. The equation that describes isotonic fluid transport is simply:

$$dv/dt = J_s \cdot S/c_s \tag{4}$$

where dv/dt represents the rate of change in volume ($cm^3 S^{-1}$), J_s the rate of net solute transport ($mol\,cm^{-2} S^{-1}$), S the epithelial surface (cm^2) and c_s the solute concentration in the absorbate ($mol\,cm^{-3}$). If the short-circuit current is taken as a measure of the active transport of a single cation, say Na^+, J_s can be calculated from:

$$J_s = 2\,I_{sc}/zF \tag{5}$$

where I_{sc} is measured in $A\,cm^{-2}$ and z, F have the usual meaning. Equation (4) can be then rewritten:

$$\frac{dv}{dt}\frac{1}{S} = \frac{2\,I_{sc}}{z\,Fc_s}. \tag{6}$$

For typical values of I_{sc} of $50\,\mu A\,cm^{-2}$ and c_s of 2×120 mM, the calculated value of $dv/dt\ 1/S$ is $16\,\mu l\,cm^{-2} h^{-1}$. This value is very close to the rate of fluid transport measured in other leaky epithelia (Diamond, 1962; Moreno, 1974) and to that recently obtained by Stern *et al.* (1985) in explants of epiblast in culture. Actual rates of volume increase in the otic vesicle throughout development are also of the same order. From data shown in Fig. 5, the rate of change in vesicular volume per unit surface can be easily calculated. Dividing the slope of the volume curve by the corresponding value of S, a figure between 1 and $5\,\mu l\,cm^{-2} h^{-1}$ is obtained. The implication is, therefore, that isotonic fluid transport can account for the volume increase observed between stages 18 and 22.

This does not imply that isotonic transport is the only force implicated in mass balance, indeed this is unlikely. Most probably a pressure gradient between the vesicular cavity and the exterior is built up as a consequence of the active volume transfer capacity of the epithelium and a finite distensibility of the wall (see Stern *et al.* 1985). For a typical apparent hydraulic conductivity of $10^{-4}\,cm\,s^{-1}\,atm^{-1}$ (House, 1974, table 9.2) a pressure of about 10 mmHg would be required to

generate that backflux to keep the net fluid transfer rate at the observed pace by hydraulic flow, in the absence of osmotic gradients.

We thank Dr F. J. García-Sancho for critical reading of the manuscript and Miss Sagrario Callejo for efficient typing. The work was partially funded by the Spanish C.A.I.C.Y.T., proj. no. 2873/83 and by Fellowship from the Real Academia de Medicina, Valladolid.

REFERENCES

BARBOSA, E., GIRALDEZ, F. & REPRESA, J. J. (1985). Transepithelial potential and resistance in the otic vesicle of the chick embryo. *J. Physiol.* **365**, 53P.

BOULPAEP, E. (1971). Electrophysiological properties of the proximal tubule: importance of cellular and intercellular transport pathways. In *Electrophysiology of Epithelial Cells* (ed. G. Giebisch), pp. 258–263. Stuttgart: Schattauer.

CREMASCHI, D., HENIN, S., MEYER, G. & BACCIOLA, T. (1977). Does Amphotericin B unmask an electrogenic Na^+ pump in rabbit gallbladder? Shift of gallbladders with negative to gallbladders with positive transepithelial p.d.'s. *J. Membrane Biol.* **34**, 55–71.

CRONE, C. (1984). Lack of selectivity to small ions in paracellular pathways in cerebral and muscle capillaries of the frog. *J. Physiol.* **353**, 317–337.

CROSS, M. H. (1973). Active sodium and chloride transport across the rabbit blastocoele wall. *Biol. Reprod.* **8**, 566–575.

DIAMOND, J. M. (1962). Mechanism of solute transport by the gallbladder. *J. Physiol.* **161**, 474–502.

FRIZZELL, R. A. & SCHULTZ, S. G. (1972). Ionic conductances of extracellular shunt pathway in rabbit ileum. *J. gen. Physiol.* **59**, 318–336.

FRIZZELL, R. A., DUGAS, M. C. & SCHULTZ, S. G. (1975). Sodium chloride transport in rabbit gallbladder. *J. gen. Physiol.* **65**, 769–795.

FRÖMTER, E. (1972). The route of passive ion movement through the epithelium of *Necturus* gallbladder. *J. Membrane Biol.* **8**, 259.

FRÖMTER, E. & DIAMOND, J. M. (1970). Route of passive ion permeation in epithelia. *Nature New Biol.* **235**, 9–13.

FRÖMTER, E., MULLER, C. W. & WICK, T. (1971). Permeability properties of proximal tubular epithelium of the rat kidney as studied with electrophysiological methods. In *Electrophysiology of Epithelial Cells* (ed. G. Giebisch), pp. 119–146. Stuttgart: Schattauer.

GIRALDEZ, F. (1984). Active sodium transport and fluid secretion in the epithelium of *Necturus* gallbladder. *J. Physiol.* **348**, 431–455.

HAMBURGER, V. & HAMILTON, H. L. (1951). A series of normal stages in the development of the chick embryo. *J. Morph.* **88**, 49–92.

HOUSE, C. R. (1974). *Water Transport in Cells and Tissues.* London: Edward Arnold Publishers Ltd.

LEDERER, W. J., SPINDLER, A. J. & EISNER, D. A. (1979). Thick slurry bevelling. *Pflügers Arch. ges. Physiol.* **381**, 287–288.

LEW, V. L. L., FERREIRA, H. G. & MOURA, T. M. (1979). The behaviour of transporting epithelial cells. I. *Proc. R. Soc.* B **206**, 53–83.

MORENO, J. H. (1974). Selective inhibition of cation conductance in "leaky" junctions of epithelia. *Nature, Lond.* **251**, 150–151.

REUSS, L. (1978). Effects of Amphotericin B on the electrical properties of *Necturus* gallbladder. Intracellular microelectrode studies. *J. Membrane Biol.* **41**, 65–86.

REUSS, L., BELLO-REUSS, E. & GRADY, T. P. (1979). Effects of ouabain on fluid transport and electrical properties of *Necturus* gallbladder. *J. gen. Physiol.* **73**, 385–402.

ROMANOFF, R. (1960). *The Avian Embryo.* New York: The MacMillan Co.

SLACK, C. & WARNER, A. E. (1973). Intracellular and intercellular potentials in the early amphibian embryo. *J. Physiol.* **232**, 313–330.

SLACK, C. & WARNER, A. E. (1975). Properties of surface and junctional membranes of embryonic cells isolated from blastula stages of *Xenopus laevis*. *J. Physiol.* **248**, 97–120.

SMITH, M. W. (1970). Active transport in the rabbit blastocyst. *Experientia* **26**, 736–738.

STERN, C. D. & MACKENZIE, D. O. (1983). Sodium transport and the control of epiblast in the early chick embryo. *J. Embryol. exp. Morph.* **77**, 73–98.

STERN, C. D., MANNING, S. & GILLESPIE, J. I. (1985). Fluid transport across the epiblast of the early chick embryo. *J. Embryol. exp. Morph.* **88**, 365–384.

VALDECASAS, J. M., BARBOSA, E., CAMPELO, E., COCA, M. C. & BARBOSA, L. (1977). Estudio ultraestructural de la placoda ótica. *An. Desarr.* **21**, 23–26.

WARNER, A. E. (1983). Physiological approaches to early development. In *Recent Advances in Physiology* (ed. P. F. Baker), pp. 87–123. London, New York: Churchill-Livingstone.

ZILLES, K. J. (1978). Ontogenesis of the visual system. In *Advances in Anatomy Embryology and Cell Biology*, vol. 54 fasc. 3. Berlin, Heidelberg, New York: Springer-Verlag.

(*Accepted 1 May 1986*)